Active Site Inhibitors Protect Protein Kinase C from Dephosphorylation and Stabilize Its Mature Form*

Christine M. Gould[‡§1], **Corina E. Antal**[‡§], **Gloria Reyes**[‡], **Maya T. Kunkel**[‡], **Ryan A. Adams**[‡2], **Ahdad Ziyar**[‡],
Tania Riveros[‡§], **and Alexandra C. Newton**[‡3]

From the ‡Department of Pharmacology and §Biomedical Sciences Graduate Program, University of California, San Diego,
La Jolla, California 92093-0721

Conformational changes acutely control protein kinase C (PKC). We have previously shown that the autoinhibitory pseudosubstrate must be removed from the active site in order for 1) PKC to be phosphorylated by its upstream kinase phosphoinositide-dependent kinase 1 (PDK-1), 2) the mature enzyme to bind and phosphorylate substrates, and 3) the mature enzyme to be dephosphorylated by phosphatases. Here we show an additional level of conformational control; binding of active site inhibitors locks PKC in a conformation in which the priming phosphorylation sites are resistant to dephosphorylation. Using homogeneously pure PKC, we show that the active site inhibitor Gö 6983 prevents the dephosphorylation by pure protein phosphatase 1 (PP1) or the hydrophobic motif phosphatase, pleckstrin homology domain leucine-rich repeat protein phosphatase (PHLPP). Consistent with results using pure proteins, treatment of cells with the competitive inhibitors Gö 6983 or bisindolylmaleimide I, but not the uncompetitive inhibitor bisindolylmaleimide IV, prevents the dephosphorylation and down-regulation of PKC induced by phorbol esters. Pulse-chase analyses reveal that active site inhibitors do not affect the net rate of priming phosphorylations of PKC; rather, they inhibit the dephosphorylation triggered by phorbol esters. These data provide a molecular explanation for the recent studies showing that active site inhibitors stabilize the phosphorylation state of protein kinases B/Akt and C.

PKC isozymes comprise a family of multidomain proteins that are under exquisite conformational control. Two major mechanisms control the conformation of PKC family members: phosphorylation and second messenger-dependent membrane binding (1, 2). First, newly synthesized enzymes undergo a series of ordered phosphorylations that lock the enzyme into a stable, catalytically competent, and autoinhibited species (3, 4). This species is maintained in an autoinhibited conformation by a pseudosubstrate segment that blocks the substrate-binding cavity, a conformation that also protects the priming sites of PKC from dephosphorylation. The inactive species are local-ized throughout the cell, often tethered to scaffold proteins (5). This processing by phosphorylation is constitutive and required to protect PKC from degradation; unphosphorylated protein is rapidly degraded (1). Second, binding to lipid second messengers allosterically controls the enzyme by facilitating the release of the autoinhibitory pseudosubstrate segment from the substrate-binding cavity (6). Thus, this conformational transition is acutely controlled by activation of receptors that signal using diacylglycerol as the second messenger. The membrane-bound conformation has an increased sensitivity to phosphatases by 2 orders of magnitude (7), and prolonged activation, as occurs with phorbol esters (functional analogues of diacylglycerol), results in the dephosphorylation and subsequent degradation of PKC (8). Thus, phosphorylation converts newly synthesized PKC into a stable, degradation-resistant conformation, and membrane binding converts PKC into a catalytically active but degradation-sensitive conformation.

The PKC family is composed of nine genes (9, 10), of which the conventional (α, the alternatively spliced βI and βII, and brain-enriched γ) and novel (δ, ϵ, η, and hematopoietic-enriched θ) isozymes are matured by phosphorylation on three conserved sites originally identified in PKC βII: the activation loop at the entrance to the active site and two C-terminal sites, the turn motif and hydrophobic motif (3). Atypical PKC isozymes (ζ and ι) are also phosphorylated at the activation loop and turn motif, but a phosphomimetic is present at the hydrophobic motif. The upstream kinase PDK-1[4] catalyzes the phosphorylation of the activation loop of all PKC isozymes, an event that correctly aligns residues in the active site for catalysis (11–13). A subset of PKC isozymes, which includes the conventional PKCs but only some of the novel PKCs (notably ϵ but not δ), is also controlled by the mammalian target of rapamycin 2 (mTORC2) complex, which is required for phosphorylation of the turn motif (14–16). PKC isozymes autophosphorylate by an intramolecular mechanism at the hydrophobic motif in vitro, but whether this mechanism regulates this site in cells has not been resolved (17, 18). Phosphorylation serves two key functions for conventional and novel PKC isozymes; it stabilizes PKC to prevent degradation, and it primes PKC to

---

[4] The abbreviations used are: PDK-1, phosphoinositide-dependent kinase 1; Bis I, bisindolylmaleimide I; Bis IV, bisindolylmaleimide IV; PDBu, phorbol 12,13-dibutyrate; PMA, phorbol 12-myristate 13-acetate; PP1, protein phosphatase 1; 1-Na-PP1, 1-naphthyl PP1; PHLPP, PH domain leucine-rich repeat protein phosphatase; PH, pleckstrin homology; mTOR, mammalian target of rapamycin; DMSO, dimethyl sulfoxide; CKAR, C kinase activity reporter.

be immediately activatable following the generation of second messengers.

Although the phosphorylation of PKC isozymes is constitutive, occurring with a half-time of ~15 min following its biosynthesis (19), the dephosphorylation of PKC is agonist-dependent. Dephosphorylated PKC is rapidly degraded by a proteasome-dependent pathway (20–22). Phorbol esters promote the "down-regulation" of PKC because they recruit PKC to membranes, expelling the pseudosubstrate and thus increasing phosphatase sensitivity. The recently discovered phosphatase PH domain leucine-rich repeat protein phosphatase (PHLPP) selectively dephosphorylates the hydrophobic motif (23), an event that shunts PKC to the detergent-insoluble fraction, where it becomes dephosphorylated at the remaining priming sites, ubiquitinated, and then ultimately degraded (8, 24). Thus, the steady-state levels of PKC are set by the balance of phosphorylation *versus* dephosphorylation. Indeed, modulation of the levels of PHLPP in mammalian cells by either overexpression or genetic silencing directly sets the levels of intracellular PKC, thus setting the gain of the PKC signal. Decreased levels of PHLPP in colon cancer cell lines have been shown to directly correlate with greatly elevated PKC levels (23). Thus, mechanisms to control the phosphorylation state of PKC impact the steady-state levels of the kinase.

Two recent studies have shown that inhibitors increase the steady-state levels of phosphorylated PKC and its close cousin, Akt (25, 26). In the case of Akt, which is not basally phosphorylated, treatment of cells with active site inhibitors increased the steady-state levels of phosphorylated Akt (25). In the case of PKC, which is constitutively phosphorylated, Parker and coworkers (26) showed that incubation of cells with active site-directed inhibitors resulted in an increase in the phosphorylation state of a catalytically impaired PKC that is not normally phosphorylated. This construct, in which the Lys that coordinates the α-β phosphates of ATP is mutated to Met or Arg, accumulates as the non-phosphorylated species under normal conditions, but accumulates as the phosphorylated species when cells are preincubated with ATP analogues such as bisindolylmaleimide I (Bis I). Whether these inhibitors increase the steady-state levels of phosphorylated PKC by increasing the rate of priming phosphorylation or by protecting phosphorylated PKC from dephosphorylation was unresolved. This latter possibility is supported by previous data showing that occupancy of the active site by the pseudosubstrate, peptide substrates, or ATP protects PKC from dephosphorylation (27–29).

Here we address the molecular mechanism by which occupancy of the active site with ATP analogues affects the phosphorylation state of PKC. We show that active site inhibitors prevent the dephosphorylation of pure protein *in vitro* and prevent the phorbol ester-mediated dephosphorylation of endogenous and overexpressed PKC in cells. Pulse-chase analysis reveals that the inhibitors do not alter the net rate of priming phosphorylations of endogenous PKC; rather, they protect from dephosphorylation.

EXPERIMENTAL PROCEDURES

Materials—Oligonucleotides were purchased from Integrated DNA Technologies. EasyTag [^{35}S]methionine/cysteine

(Met/Cys, 1175 Ci mmol^{-1}) was purchased from PerkinElmer Life Sciences. Met/Cys-deficient DMEM was purchased from Invitrogen. Carbobenzoxy-L-leucyl-L-leucyl-L-leucinal (MG-132), phorbol 12-myristate 13-acetate (PMA), phorbol 12,13-dibutyrate (PDBu), Gö 6983, bisindolylmaleimide IV (Bis IV), and chelerythrine were purchased from Calbiochem. Bis I (also known as BIM) was purchased from Alexis Biochemicals. 1-Na-PP1 was a generous gift from Kavita Shah (Purdue University). Purified PKC βII (3580 units mg^{-1}) was purchased from Millipore; GST-tagged PKC α from baculovirally infected Sf-9 cells was purified to homogeneity by GST affinity chromatography using the Profinia protein purification system (Bio-Rad). The catalytic subunit of protein phosphatase 1 (PP1) (2500 units ml^{-1}) was purchased from New England Biolabs. A polyclonal antibody to PKC βII was obtained from Santa Cruz Biotechnology. Monoclonal antibodies to PKC α and PKC β were obtained from BD Transduction Laboratories. The phospho-Ser PKC substrate antibody was purchased from Cell Signaling, and the monoclonal anti-β-actin antibody was purchased from Sigma-Aldrich. UltraLink protein A/G beads were obtained from Thermo Scientific. All other materials and chemicals were reagent grade.

Plasmid Constructs, Cell Culture, and Transfection—All PKC mutants, PKC βII-D466N, PKC βII-T500E, PKC βII-D466N/T500E, PKC βII-F629A, and PKC α-M417G, were generated by QuikChange site-directed mutagenesis (Stratagene). COS7 cells were maintained in DMEM (Cellgro) containing 10% fetal bovine serum (HyClone) and 1% penicillin/streptomycin at 37 °C in 5% CO$_2$. Transient transfection of COS7 cells was carried out using the FuGENE 6 transfection reagent (Roche Applied Science) or the jetPRIME transfection reagent (PolyPlus Transfection).

Phosphatase Incubations—Homogeneously pure PKC βII (50 nM) was incubated with the catalytic subunit of PP1 (25 units ml^{-1}) in 20 mM HEPES buffer, pH 7.5, containing 200 μM MnCl$_2$, 1 mM DTT, 0.5 mM CaCl$_2$, and 0.04 mM EDTA in the presence or absence of 140 μM phosphatidylserine/4 μM diacylglycerol for 20 min at 22 °C. Where indicated, reactions were carried out in the presence of 6 μM Gö 6983. Reactions were quenched by the addition of SDS-PAGE sample buffer and analyzed by SDS-PAGE (7.5% acrylamide) and Western blotting using a monoclonal antibody for PKC βII (BD Transduction Laboratories) that labels phosphorylated and unphosphorylated PKC βII equally well.

GST-tagged PKC α (3.6 × 10^{-3} μg/μl) and GST-tagged PHLPP2-PP2C were incubated in 10 mM Tris, pH 7.4, containing 1 mM CaCl$_2$, 140 μM phosphatidylserine/4 μM diacylglycerol, 2 mM MnCl$_2$, 0.3 μM BSA, and protease inhibitors (0.04 mg/ml leupeptin, 2 mM benzamidine, 2 mM DTT, and 0.2 mM PMSF) in the presence or absence of 6 μM Gö 6983 at room temperature. Aliquots were removed at the indicated times and stopped by the addition of SDS-PAGE sample buffer. Relative dephosphorylation of GST-PKC α was assessed by Western blotting and probing for total PKC α and Ser(P)-657 phosphorylation followed by incubation with peroxidase-conjugated secondary antibodies and chemiluminescence for detection.

Phorbol Ester and Inhibitor Treatment of Cells—COS7 cells were transiently transfected with WT PKC βII. Approximately

24 h after transfection, cells were pretreated with 1 μM Gö 6983 or 10 μM MG-132 for 30 min prior to stimulation with 200 nM PMA for the indicated times. The cells were lysed in Buffer A (50 mM Tris, pH 7.4, 1% Triton X-100, 50 mM NaF, 10 mM Na$_4$P$_2$O$_7$, 100 mM NaCl, 5 mM EDTA, 1 mM Na$_3$VO$_4$, and 1 mM PMSF), and whole cell lysates were analyzed by SDS-PAGE and Western blotting. For inhibitor incubations with Gö 6983 and Bis IV, COS7 cells transiently expressing WT PKC βII or PKC βII-F629A were treated with 6 μM Gö 6983, 6 μM Bis IV or DMSO for 30 min prior to stimulation with 200 nM PDBu for the indicated times. Whole cell lysates were collected and analyzed by SDS-PAGE and Western blotting. For inhibitor experiments with chelerythrine and Gö 6976, COS7 cells were pretreated for 15 min with the indicated concentrations of chelerythrine, 500 nM Gö 6976, or vehicle (DMSO) and then treated with 200 nM PMA for 15 min. Whole cell lysates were analyzed by SDS-PAGE and Western blotting.

FRET Imaging and Analysis—COS7 cells were rinsed with and imaged in Hanks' balanced salt solution (Cellgro) supplemented with 1 mM CaCl$_2$. For the chelerythrine experiments, cells were pretreated with inhibitor for 30 min prior to imaging. CFP, YFP, and FRET images were acquired and analyzed as described previously (30). Base-line images were acquired for 5 or more min before ligand addition. Individual data traces were normalized to 1 by dividing by the average base-line FRET ratio, and data from at least three different imaging dishes were referenced around the ligand addition time point. The normalized average FRET ratio is the average of these corrected values $\pm$ S.E.

Statistical Analysis—Statistical analysis was performed using the JMP statistical software, version 9 (SAS Institute Inc., Cary, NC).

Pulse-Chase Analysis—COS7 cells were transfected with WT PKC βII or PKC βII-D466N. At 24–30 h after transfection, cells were incubated with Met/Cys-deficient DMEM for 30 min at 37 °C. The cells were then pulse-labeled with 0.5 mCi ml^{-1} [^{35}S]Met/Cys in Met/Cys-deficient DMEM for 7 min at 37 °C, medium was removed, and cells were chased with DMEM containing 10% fetal bovine serum and 1% penicillin/streptomycin. At the indicated times, cells were lysed in Buffer A and centrifuged at 16,000 $\times$ g for 5 min at 22 °C, and PKC βII in the supernatant was immunoprecipitated with an anti-PKC α monoclonal antibody (cross-reactive with PKC βII) overnight at 4 °C. The immune complexes were collected with UltraLink protein A/G beads, washed with Buffer A, separated by SDS-PAGE, transferred to PVDF membrane, and analyzed by autoradiography. For the inhibitor experiments with MG-132 and Gö 6983, cells were chased in the presence of 10 μM MG-132 or 1 μM Gö 6983 for 90 min and then treated with 200 nM PMA for 4 h. For the Bis I inhibitor/PMA experiment, cells were chased in the presence of 2 μM Bis I, and then at 90 min of chase, cells were treated with 200 nM PMA for the indicated times.

RESULTS

Two recent studies reveal that treatment of cells with active site-directed inhibitors of PKC or Akt paradoxically increases the phosphorylation state of these kinases (25, 26). To understand the molecular mechanism driving the increase in steady-
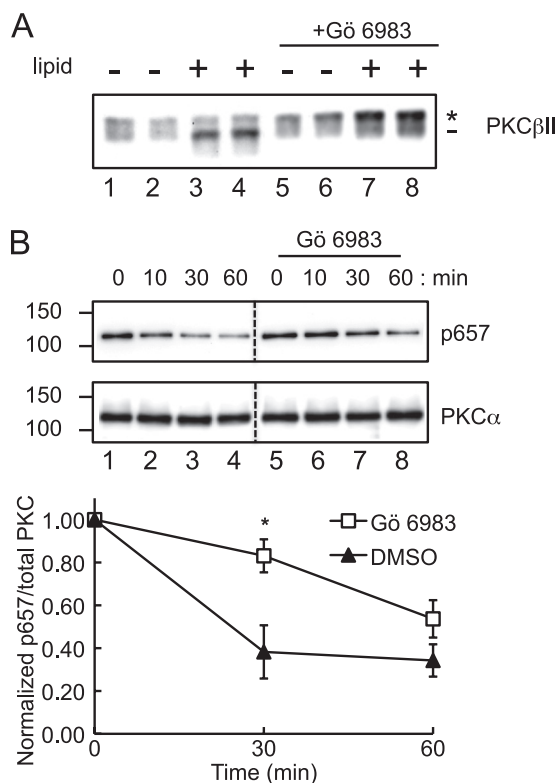

FIGURE 1. **Kinase inhibitors protect PKC from dephosphorylation *in vitro* and in cells.** *A*, pure PKC βII was incubated with PP1 in the absence (*lanes 1–4*) or presence (*lanes 5–8*) of 6 μM Gö 6983, either in the absence (*lanes 1, 2, 5,* and *6*) or in the presence (*lanes 3, 4, 7,* and *8*) of the PKC activators, phosphatidylserine/diacylglycerol and Ca^{2+}, and analyzed by SDS-PAGE and Western blotting for PKC βII. The *asterisk* indicates the position of fully phosphorylated PKC, and the *dash* denotes the position of PKC dephosphorylated at all three priming sites. *B*, pure GST-PKC α was incubated with pure GST-PHLPP2-PP2C in the absence (*lanes 1–4*) or presence (*lanes 5–8*) of 6 μM Gö 6983 for the indicated times and analyzed by SDS-PAGE and Western blotting for PKC α and Ser(P)-657 phosphorylation. A graph depicting the average p657/total PKC α ratio normalized to the 0-min time point for three independent experiments is shown below. *Error bars* represent S.E. *, *p* < 0.05 as determined by a Students' *t* test.

state phosphorylation levels, we asked whether binding of inhibitors 1) increases the maturation rate of PKC or 2) decreases susceptibility of PKC to dephosphorylation.

First, we examined whether binding of active site inhibitors alters the sensitivity of PKC βII to dephosphorylation. We focused on PKC βII because its maturation by phosphorylation and its dephosphorylation have been extensively studied (3). Pure PKC βII (from baculovirus expression and thus quantitatively phosphorylated at C-terminal sites and approximately half-phosphorylated at the activation loop site (17)) was incubated with pure PP1, either in the presence or in the absence of activating lipids (phosphatidylserine/diacylglycerol) and Ca^{2+} and in the presence or absence of the active site inhibitor Gö 6983. This phosphatase removes all three priming sites of PKC (17). Dephosphorylation of PKC βII was assessed by monitoring the mobility shift on SDS-PAGE that accompanies loss of the two C-terminal phosphorylations (7, 17). The Western blot in Fig. 1*A* shows that PKC βII was effectively dephosphorylated by PP1 in the membrane-bound conformation (activating conditions, *lanes 3* and *4*; faster mobility species lacking phosphates at the turn motif and hydrophobic motif is indicated by

the *dash*) but not in the inactive conformation (absence of lipid/ Ca^{2+}, *lanes 1* and *2*; slower mobility species that is quantitatively phosphorylated at the two C-terminal sites is indicated by the *asterisk*). This result is consistent with our previous studies showing that membrane binding increases the rate of PP1-catalyzed dephosphorylation of PKC by 2 orders of magnitude (7). Importantly, preincubation with Gö 6983 blocked the dephosphorylation of membrane-bound PKC βII; phosphatase treatment did not result in significant dephosphorylation of PKC βII either in the absence (*lanes 5* and *6*) or in the presence (*lanes 7* and *8*) of lipid and Ca^{2+}. These concentrations of Gö 6983 had no effect on the intrinsic activity of PP1 as assessed by dephosphorylation of the substrate *p*-nitrophenyl phosphate (data not shown); we have previously shown that lipid/Ca^{2+} do not affect the catalytic activity of PP1 (7). Thus, these data reveal that occupancy of the active site of PKC βII with an active site-directed inhibitor, Gö 6983, locks the enzyme in a more phosphatase-resistant conformation.

We next tested whether inhibitor binding also protects PKC from dephosphorylation by PHLPP, the physiological phosphatase that catalyzes the first step in the dephosphorylation of PKC (23): removal of the hydrophobic motif phosphate. Pure PKC α was incubated with the purified phosphatase domain of PHLPP2, under activating conditions, and the dephosphorylation of the hydrophobic motif (Ser-657) was monitored with a phospho-specific antibody. Quantification of the Western blot in Fig. 1*B* reveals that Gö 6983 reduced the rate of dephosphorylation by PHLPP ~4-fold. These data support the finding that phosphatase protection by active site inhibitors is an inherent property of the kinase.

We next addressed the effect of Gö 6983 on the dephosphorylation of PKC in cells. Dephosphorylation was triggered by treating cells with the phorbol ester, PMA, a potent activator of PKC. Fig. 2*A* shows that PKC βII expressed in COS7 cells migrates as an upper mobility band (*lane 1*, *asterisk*), reflecting quantitative phosphorylation at the two C-terminal sites. Treatment with PMA for 3 h resulted in the accumulation of dephosphorylated PKC (*lane 5*, faster electrophoretic mobility is indicated by the *dash*), which represents PKC quantitatively dephosphorylated at both C-terminal sites (17); an intermediate band reflecting loss of phosphate at only one of the C-terminal sites was not observed. Loss of the activation loop phosphate also occurred with identical kinetics as loss of the C-terminal sites; Western blot analysis with a phospho-specific antibody to the activation loop site (Thr-500) revealed that the ratio of phospho-signal to total PKC migrating with the slower mobility was 1:1 for all time points (data not shown). Thus, all three priming sites are lost simultaneously. Treatment for 6 h (*lanes 9–12*) resulted in almost complete dephosphorylation (*lane 9*, *dash*). However, pretreatment of cells with the PKC inhibitor Gö 6983 resulted in a marked reduction in phorbol ester-triggered dephosphorylation as assessed by the trapping of upper mobility (phosphorylated) PKC (*lane 10*, *asterisk*). Specifically, the amount of phosphorylated PKC increased 2.5-fold from ~30% in the absence of Gö 6983 (*lane 5*) to ~73% in the presence of inhibitor (*lane 6*) following 3 h of phorbol ester treatment and from virtually undetectable (<10%) in the absence of inhibitor (*lane 9*) to ~60% in the presence of inhib-
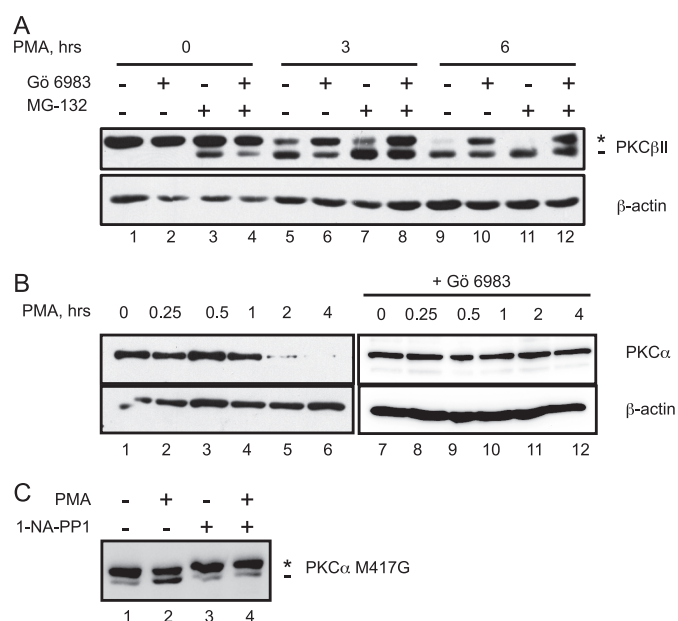

FIGURE 2. **Kinase inhibitors protect PKC from phorbol ester-mediated down-regulation and degradation.** *A*, COS7 cells were transiently transfected with WT PKC βII and either treated with 200 nM PMA alone (*lanes 1, 5, and 9*) or pretreated with 10 μM MG-132 (*lanes 3, 7,* and *11*) or 1 μM Gö 6983 (*lanes 2, 6,* and *10*) or both (*lanes 4, 8,* and *12*) prior to PMA stimulation for the indicated times. Whole cell lysates were analyzed by SDS-PAGE and Western blotting for total PKC (PKC βII) and total protein (β-actin). The *asterisk* denotes the position of phosphorylated PKC, and the *dash* denotes the position of unphosphorylated PKC. *B*, COS7 cells were treated with PMA alone (200 nM, *lanes 1–6*) or in the presence of the PKC inhibitor Gö 6983 (1 μM, *lanes 7–12*) for the indicated times. Whole cell lysates were analyzed by SDS-PAGE and Western blotting for total PKC (PKC α) and total protein (β-actin). *C*, COS7 cells were transiently transfected with PKC α M417G and untreated (*lane 1*), treated with 200 nM PMA (*lane 2*), treated with 1 mM 1-Na-PP1 alone (*lane 3*), or pretreated with 1-Na-PP1 followed by PMA (*lane 4*). Cell lysates were analyzed by SDS-PAGE and Western blotting for total PKC. The *asterisk* denotes the position of phosphorylated PKC, and the *dash* denotes the position of unphosphorylated PKC.

itor (*lane 10*) following 6 h of phorbol ester treatment. We also examined the effect of Gö 6983 on the phorbol ester-mediated dephosphorylation in the presence of the proteasome inhibitor, MG-132, to prevent degradation of the dephosphorylated species of PKC. Treatment of cells with the proteasome inhibitor resulted in accumulation of dephosphorylated PKC, with modest accumulation (~10% of total PKC) observed even in the absence of phorbol ester stimulation (*lane 3*, *dash*); this reveals a role of proteasomal degradation in maintaining the basal steady-state levels of PKC. Pretreatment with the active site inhibitor Gö 6983 reduced the amount of basally dephosphorylated PKC (compare the intensity of the faster migrating band (*dash*) in *lanes 3* and *4*) and more effectively trapped the phosphorylated species when compared with cells in which the proteasome was not inhibited (compare the intensity of the slower migrating band (*asterisk*) in *lanes 6* and *8* and *lanes 10* and *12*). Thus, treatment with Gö 6983 prevents the phorbol ester-dependent dephosphorylation of PKC (upper band accumulation), and treatment with MG-132 prevents the degradation of dephosphorylated PKC (lower band accumulation).

To investigate whether Gö 6983 affects the rate of down-regulation of endogenous PKC, COS7 cells were pretreated with or without Gö 6983 and stimulated with PMA, and the total protein levels of the predominant conventional isozyme in

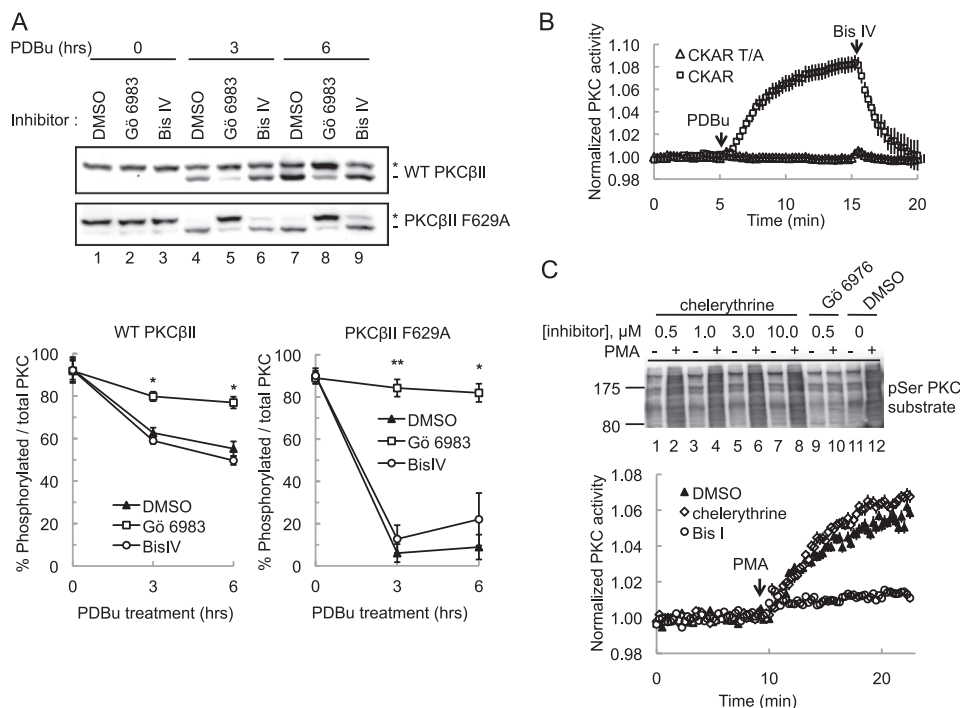# Inhibitors Block Protein Kinase C Dephosphorylation

FIGURE 3. **Active site occupancy, not inhibition of activity, protects PKC from dephosphorylation.** *A,* COS7 cells transiently transfected with either WT PKC βII or PKC βII-F629A were pretreated with DMSO, Gö 6983, or Bis IV for 30 min prior to stimulation with 200 nM PDBu for 3 or 6 h. Whole cell lysates were analyzed by SDS-PAGE and Western blotting for total PKC (PKC β). The *asterisk* denotes the position of mature, fully phosphorylated PKC, and the *dash* denotes the position of unphosphorylated PKC. Representative blots are shown on the *top.* Quantitative analysis of data representing the percentage of phosphorylated PKC (*upper band*) divided by total PKC (*upper* and *lower bands*) are shown on the *bottom.* Data represent the mean $\pm$ S.E. of three independent experiments. Statistical significance was determined by a one-way analysis of variance followed by Dunnett's post hoc tests in the comparison of DMSO control *versus* each inhibitor treatment. *Double* and *single asterisks* indicate significant difference at $p < 0.01$ and $p < 0.05$, respectively. *B,* COS7 cells were transiently transfected with CKAR (*squares*) or CKAR T/A (*triangles*), a reporter lacking the phospho-acceptor site. The average normalized FRET ratio is shown as a function of time following the addition of 200 nM PDBu and then the PKC inhibitor Bis IV at the indicated time points. Data represent the mean $\pm$ S.E. of three independent experiments referenced around the ligand addition time point. *C,* COS7 cells were pretreated for 15 min with the indicated concentrations of chelerythrine, 500 nM Gö 6976, or vehicle (DMSO), treated with 200 nM PMA for 15 min, and then lysed and analyzed by SDS-PAGE and Western blotting with a phospho-Ser PKC (*pSer PKC*) substrate antibody (*top*). COS7 cells transfected with CKAR and pretreated with vehicle (DMSO, *triangles*), 500 nM chelerythrine (*diamonds*), or 500 nM Bis I (*circles*) were monitored for changes in FRET in response to 200 nM PMA (mean $\pm$ S.E. for $n \geq 11$ per group) (*bottom*).

these cells, PKC α, were examined by Western blot analysis. Note that the rate-limiting step in the down-regulation of endogenous PKC α is the hydrophobic motif dephosphorylation step, and consequently, no dephosphorylated intermediate is observed (it is rapidly degraded) (23). Thus, we examined the disappearance of the upper mobility, fully phosphorylated species. The Western blot in Fig. 2B shows that PMA treatment resulted in the quantitative disappearance of phosphorylated PKC within 4 h, with a half-time of $\sim$1 h (*lanes 1–6*). Strikingly, Gö 6983 pretreatment of cells protected PKC from PMA-induced down-regulation, with no significant reduction in the level of phosphorylated enzyme observed following 4 h of PMA treatment (compare *lanes 7* and *12*). As reported by Parker and co-workers (26) for PKC ϵ, similar protection from down-regulation was also observed for the binding of the bulky inhibitor 1-Na-PP1 to a gatekeeper construct of PKC α-M417G whose active site was enlarged to accommodate this inhibitor (31) (Fig. 2C, compare *lanes 2* and *4*). Taken together, these data reveal that active site inhibitors prevent the dephosphorylation and subsequent degradation of endogenous, conventional PKC α as well as overexpressed enzyme.

To ensure that the protection from dephosphorylation observed in cells occurred due to active site occupancy, rather than because the activity of PKC is required for its dephosphorylation, we examined the effect of an uncompetitive inhibitor

on phorbol ester-dependent dephosphorylation. COS7 cells overexpressing PKC βII were pretreated with DMSO, Gö 6983, or the uncompetitive inhibitor Bis IV (32) and then treated with the phorbol ester PDBu for 3 or 6 h. PDBu triggered the dephosphorylation of PKC βII as assessed by the appearance of the faster migrating band (Fig. 3A, *lanes 4* and *7, dash*), and this dephosphorylation was prevented by pretreatment with Gö 6983 (Fig. 3A, *lanes 5* and *8*). In striking contrast, Bis IV pretreatment had no effect on the rate of PDBu-triggered dephosphorylation (Fig. 3A, *graph*). This protection from dephosphorylation was exaggerated in cells overexpressing a PKC βII construct containing a destabilizing mutation within the highly conserved NFD motif of the AGC protein kinase family, corresponding to F629A in PKC βII (33–35). This construct was more readily down-regulated by PDBu when compared with wild-type enzyme (Fig. 3A, compare *lane 1* with *lanes 4* and *7*). However, when Gö 6983 was bound in the active site, PKC βII-F629A was protected from dephosphorylation (*lanes 5* and *8, asterisk*); the uncompetitive inhibitor Bis IV did not protect from dephosphorylation (*lanes 6* and *9, graph*). Bis IV effectively inhibited cellular PKC as assessed by its ability to reverse the PDBu-stimulated FRET change of the genetically encoded C kinase activity reporter, CKAR, whereas it had no effect on CKAR T/A, a reporter lacking the phospho-acceptor site (Fig. 3B). Note that Parker and co-workers (26) reported that chel-

erythrine does not alter the steady-state phosphorylation of PKC and used this result to argue that only active site inhibitors alter the steady-state phosphorylation of PKC. Although chelerythrine is marketed as a PKC inhibitor, Cohen and co-workers (36) report that it does not inhibit pure PKC isozymes (nor any of 34 structurally diverse kinases in their inhibitor screen). Because it is so commonly used as a PKC inhibitor, we directly tested its ability to inhibit PKC activity in cells. The Western blot in Fig. 3*C* shows that pretreatment of COS7 cells with up to 10 μM chelerythrine had no effect on the PMA-induced phosphorylation of PKC substrates as assessed using a phospho-Ser PKC substrate antibody (compare *lanes 7* and *8*); in contrast, 0.5 μM Gö 6976 abolished the phorbol ester-dependent increase in immunoreactivity (compare *lanes 9* and *10*). Consistent with this result, pretreatment of COS7 cells with chelerythrine had no effect on the PMA-dependent increase in PKC activity reported by CKAR (Fig. 3*C*, *diamonds*). This increase in activity was effectively prevented by Bis I (Fig. 3*C*, *circles*), another active site inhibitor that was used in the study by Parker and co-workers (26) and that differs from Gö 6893 by only one substituent, a methyl ether (37). Thus, the uncompetitive inhibitor Bis IV is the more appropriate pharmacological agent to inhibit cellular PKC in a manner that does not involve competitive binding to active site. Using Bis IV, we establish that the protection from dephosphorylation by Gö 6983 is not through inhibition of PKC activity, but rather from occupancy of the active site to lock the enzyme in a phosphatase-resistant conformation.

As a final test to unequivocally establish that active site inhibitors, such as Gö 6983, affect the steady-state levels of PKC phosphorylation by preventing dephosphorylation, rather than accelerating phosphorylation, we used a pulse-chase analysis to determine the rate of phosphorylation and the subsequent rate of phorbol ester-triggered dephosphorylation of a pool of newly synthesized PKC (26). Bis I did not accelerate the rate of phosphorylation of PKC; half of the newly synthesized pool had matured to the fully phosphorylated species 15 min following the chase (Fig. 4*A*, *lanes 2* and *9*). Rather, Bis I significantly slowed the phorbol ester-triggered dephosphorylation of matured PKC; the half-time for dephosphorylation of PKC was 2.9 $\pm$ 0.7 h in the absence of Bis I (Fig. 4*B*, *circles*) and 6.5 $\pm$ 0.8 h in the presence of Bis I (Fig. 4*B*, *squares*). These data reveal that occupancy of the active site does not promote the phosphorylation of PKC; rather, it inhibits the dephosphorylation of PKC.

Pure PKC βII autophosphorylates by an intramolecular reaction *in vitro* at the hydrophobic motif site (7, 17, 18). Whether this mechanism drives the phosphorylation in cells has been the subject of debate. The use of pharmacological inhibitors to address the mechanism in cells is compromised by our recent finding that the activities of both PKC and PDK-1 are refractory to pharmacological inhibition when scaffolded near their substrates (32). Notably, the priming phosphorylation of wild-type PKC by PDK-1 is insensitive to the PDK-1 inhibitors OSU03012 and KT5720. Similarly, the net rate of priming phosphorylations of PKC is insensitive to the PKC inhibitor Bis I (Fig. 4*A*). If the phosphorylation in cells also proceeds by an intramolecular mechanism, the event may also be insensitive to inhibitors of PKC. Thus, a second approach to address whether
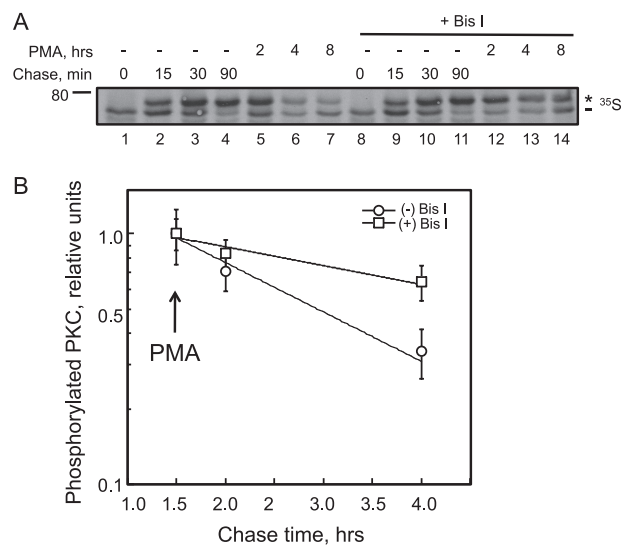

FIGURE 4. **Kinase inhibitors do not promote the processing of PKC by phosphorylation.** *A*, autoradiogram from a pulse-chase analysis of COS7 cells transfected with WT PKC βII. Transfected cells were labeled with [^{35}S]Met/Cys (^{35}S) and chased for the indicated times in the absence (*lanes 1–7*) or presence (*lanes 8–14*) of 2 μM Bis I. At 90 min of chase (*lanes 4-7* and *lanes 11–14*), cells were treated with 200 nM PMA for the indicated times. PKC was immunoprecipitated from detergent-solubilized lysates and analyzed by SDS-PAGE and autoradiography. The *asterisk* denotes the position of mature, fully phosphorylated PKC, and the *dash* denotes the position of unphosphorylated PKC (either newly synthesized as in *lane 1* or dephosphorylated as in *lane 5*). *B*, quantitative analysis of data from three independent experiments showing the rate of dephosphorylation of the pool of pulse-labeled PKC as a function of time following the addition of phorbol esters. Data represent the amount of the fully phosphorylated species at 0, 2, and 4 h of PMA, with PMA added after 1.5 h of chase (*i.e.* Fig. 2*A*, *upper band* indicated with an *asterisk*) normalized to the amount of fully phosphorylated species at 1.5 h when PMA was added. Data are shown for a pulse-chase in the absence (*circles*) or presence (*squares*) of Bis I. *Error bars* represent S.E.

PKC autophosphorylates in cells would be the use of kinase-inactive constructs. In this regard, Parker and co-workers (26) reported that mutation of the conserved Asp in PKC ϵ (Asp-532), which acts as the catalytic base in the transphosphorylation reaction but makes no contacts with the ATP, results in a catalytically inactive kinase that is still processed by phosphorylation, leading the authors to conclude that PKC does not autophosphorylate in cells. However, it has recently been shown that an analogous Asp to Asn substitution permits autophosphorylation. Lemmon and co-workers (38) recently established that the apparently kinase-inactive ErbB3/HER3, which has been considered a pseudokinase because of a natural replacement of the catalytic base Asp for Asn, is unable to phosphorylate substrates but autophosphorylates.

To explore a potential involvement of autophosphorylation in the priming phosphorylations of PKC, we examined the processing of the Asp to Asn PKC βII construct, PKC βII-D466N, by pulse-chase analysis. Fig. 5 shows that it is processed by phosphorylation at a rate comparable with wild-type enzyme (*e.g.* compare *lanes 2* and *6*, where ratios of *upper* and *lower bands* are approximately equal). One possibility is that PKC is phosphorylated by a Gö 6983-insensitive kinase at the two C-terminal sites. However, given how efficiently PKC autophosphorylates at the hydrophobic motif *in vitro*, it is also possible that PKC autophosphorylates at the hydrophobic motif in the cell but at a rate that is much faster than the rate-limiting
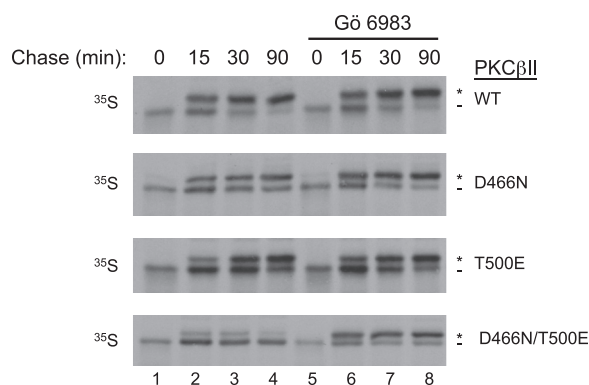
FIGURE 5. **Phosphomimetic at activation loop slows maturation sufficiently to unveil requirement of intrinsic catalytic activity in maturation.** An autoradiogram from a pulse-chase analysis of COS7 cells transfected with WT PKC βII (*top panel*), PKC βII-D466N (*second panel*), PKC βII-T500E (*third panel*), or PKC βII-D466N/T500E (*bottom panel*) is shown. Transfected cells were labeled with [^{35}S]Met/Cys (^{35}S) and chased for the indicated times in the absence (*lanes 1–4*) or presence (*lanes 5–8*) of 1 μM Gö 6983. PKC was immunoprecipitated from detergent-solubilized lysates and analyzed by SDS-PAGE and autoradiography. The *asterisk* denotes the position of mature, fully phosphorylated PKC, and the *dash* denotes the position of unphosphorylated PKC.

FIGURE 6. **Structure of PKC βII showing priming phosphorylation sites relative to active site.** A ribbon diagram representation of the catalytic domain of PKC βII as determined by Grant and co-workers (33) displays the three priming phosphorylation sites in space-filling representation: the activation loop site (Thr-500; *pink*) at the entrance to the active site and the two C-terminal sites, the turn motif (Thr-641; *orange*) and the hydrophobic motif (Ser-660; *green*). The C-terminal tail is highlighted in *dark blue*.

step in the processing of PKC. Thus, if the D466N has compromised activity, it may be invisible in our assay because this compromised activity is still faster than the rate-limiting step. To address this, we attempted to destabilize PKC so that impairing its catalytic activity (with the Asp to Asn mutation) would slow potential autophosphorylation sufficiently to make this step rate-limiting. Substitution of a Glu for the activation loop Thr that is modified by PDK-1 results in a slight loss in stability; pulse-chase analysis reveals that the T500E construct is processed at a slightly slower rate than the wild-type enzyme. When the kinase-impairing mutation is introduced on top of the T500E mutation, the processing of PKC is effectively inhibited. Thus, the effect of impairing catalytic activity on the wild-type enzyme is invisible because the residual activity is sufficiently high. However, impairing the catalytic activity on a slightly less stable construct of PKC (T500E) unveils a robust role for the catalytic activity of PKC in its C-terminal phosphorylations. These data are consistent with a model in which the rate-limiting step in the processing of PKC is so slow relative to the rate of autophosphorylation of the hydrophobic motif that impairing the catalytic activity of PKC does not affect the rate of maturation. However, destabilizing PKC by an additional mechanism (phosphomimetic at activation loop instead of phospho-Thr) unmasks a greatly reduced ability of the catalytically impaired D466N construct to undergo C-terminal phosphorylation when compared with enzyme, which is not catalytically impaired by mutation of this site. These data support a model in which intramolecular autophosphorylation also accounts for the mechanism of phosphorylation of the hydrophobic motif in cells.

The balance between phosphorylation and dephosphorylation in the maturation of PKC is evidenced on the D466N/T500E construct. Although occupancy of the active site with Gö 6983 does not affect the rate of maturation of PKC under conditions where C-terminal processing is not rate-limiting (*e.g.* WT, D466N, T500E), Gö 6983 increases the apparent rate
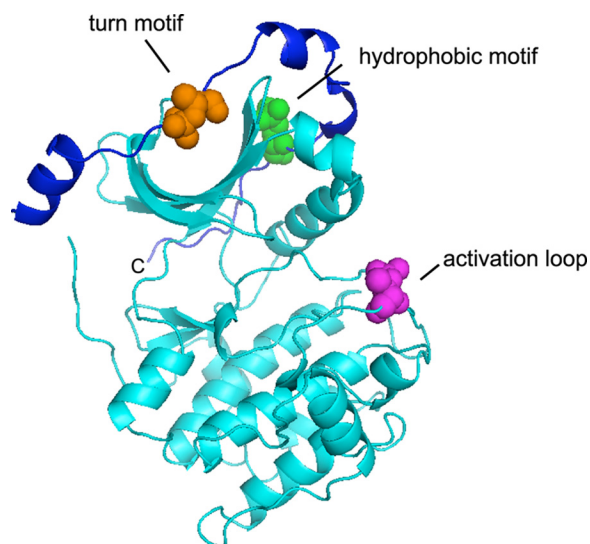
of C-terminal processing of the maturation-defective D466N/T500E construct. One explanation consistent with the finding that active site occupancy confers phosphatase resistance is that any phosphate that gets incorporated on the C-terminal sites is immediately trapped there. For the wild-type enzyme, such acceleration cannot be observed because the rate-limiting step precedes the C-terminal phosphorylation steps. However, for constructs in which catalytic activity is substantially compromised (*e.g.* D466N/T500E in this study, but also K371R (26)), suppressing the dephosphorylation opposition in processing allows kinase-impaired constructs to accumulate phosphate.

DISCUSSION

Here we show that the binding of active site inhibitors protects the priming phosphorylations of PKC from dephosphorylation. This provides a molecular explanation for the paradoxical finding that active site inhibitors increase the steady-state levels of phosphorylated PKC, a mechanism that could also account for a similar finding with Akt (25). The finding that active site occupancy protects from dephosphorylation is consistent with previous studies showing that occupancy of the active site by pseudosubstrate, peptide substrate, or Mg^{2+}-ATP protects from dephosphorylation (7, 27–29). Thus, occupancy of the active site (by pseudosubstrate segment, substrate, or inhibitors) protects the priming sites from dephosphorylation.

The first and rate-limiting step in the dephosphorylation of PKC is the removal of the hydrophobic motif phosphate by PHLPP (23). Here we show that active site inhibitors prevent this dephosphorylation both with pure proteins *in vitro* and in the context of phorbol ester-mediated dephosphorylation in cells. It is noteworthy that this site, along with the turn motif, is distal to the active site, revealing remarkable conformational restraints at these sites (Fig. 6). The finding that active site

inhibitors lock the phosphorylation sites on the C-terminal tail in a phosphatase-resistant conformation is consistent with structural studies of PKA that showed that the C-terminal tail is highly ordered when inhibitor is bound and highly disordered in the apo structure (39, 40). It is interesting to note that occupancy of the active site by ATP analogues such as Bis I expels the autoinhibitory pseudosubstrate from the substrate-binding cavity (32), an event that, in itself, increases the phosphatase sensitivity of PKC by 2 orders of magnitude (7). Thus, the protection incurred by inhibitors such as Bis I is all the more striking and underscores the conformational constraint of the phosphorylation sites upon occupancy of the active site.

Our data also support a model in which the dephosphorylation of PKC precedes its degradation (8, 23, 24). Specifically, using phorbol esters to stimulate the down-regulation of conventional PKC isozymes, we show that occupancy of the active site by ATP analogues results in the accumulation of fully phosphorylated (but not unphosphorylated) conventional PKC βII, whereas inhibition of the proteasome results in accumulation of the unphosphorylated (but not phosphorylated) species of PKC βII.

Our data also support a model in which the first and rate-limiting step in the maturation of PKC is relatively slow (pulse-chase experiments reveal a half-time of ~10–30 min for endogenous PKC α and overexpressed PKC βII (Fig. 4A) (19)). This rate-limiting step is also highly sensitive to mTOR inhibitors, suggesting that one of the mTOR complexes, mTORC2, controls the first step in the maturation of PKC.[5] Given that hydrophobic motif phosphorylation is considerably faster than the first and rate-limiting step in the maturation of PKC, neither inhibition of wild-type PKC nor the use of kinase-inactive constructs is able to resolve the question of whether PKC autophosphorylates at the hydrophobic motif in cells. However, here we show that the maturation of a T500E construct of PKC βII, in which the activation loop phospho-Thr is replaced with a less optimal phosphomimetic, is regulated by the intrinsic catalytic activity of the kinase; the D466N/T500E is not effectively processed by phosphorylation, whereas the T500E is. Thus, the finding that the D466N mutation is not processed by phosphorylation in the context of the T500E construct is consistent with the possibility that the hydrophobic motif is controlled by autophosphorylation in cells, as it is *in vitro*.

In summary, our data reveal that active site inhibitors do not promote the maturation of PKC (26). Rather, they prevent its dephosphorylation. In addition, our data, taken together with the recent finding that the Erb3/HER3 kinase, which has a natural Asp to Asn mutation replacing the catalytic base (38), autophosphorylates, continue to support a model in which the last step in the priming phosphorylations of PKC occurs by intramolecular autophosphorylation.

---

[5] G. Reyes, C. M. Gould, and A. C. Newton, unpublished data.

REFERENCES

1. Newton, A. C. (2010) *Am. J. Physiol. Endocrinol. Metab.* **298,** E395–E402
2. Griner, E. M., and Kazanietz, M. G. (2007) *Nat. Rev. Cancer* **7,** 281–294
3. Newton, A. C. (2003) *Biochem. J.* **370,** 361–371
4. Cameron, A. J., De Rycker, M., Calleja, V., Alcor, D., Kjaer, S., Kostelecky, B., Saurin, A., Faisal, A., Laguerre, M., Hemmings, B. A., McDonald, N., Larijani, B., and Parker, P. J. (2007) *Biochem. Soc. Trans.* **35,** 1013–1017
5. Schechtman, D., and Mochly-Rosen, D. (2001) *Oncogene* **20,** 6339–6347
6. Newton, A. C. (2009) *J. Lipid Res.* **50,** (suppl.) S266–S271
7. Dutil, E. M., Keranen, L. M., DePaoli-Roach, A. A., and Newton, A. C. (1994) *J. Biol. Chem.* **269,** 29359–29362
8. Hansra, G., Garcia-Paramio, P., Prevostel, C., Whelan, R. D., Bornancin, F., and Parker, P. J. (1999) *Biochem. J.* **342,** 337–344
9. Sossin, W. S. (2007) *Learn. Mem.* **14,** 236–246
10. Parker, P. J., and Murray-Rust, J. (2004) *J. Cell Sci.* **117,** 131–132
11. Le Good, J. A., Ziegler, W. H., Parekh, D. B., Alessi, D. R., Cohen, P., and Parker, P. J. (1998) *Science* **281,** 2042–2045
12. Dutil, E. M., Toker, A., and Newton, A. C. (1998) *Curr. Biol.* **8,** 1366–1375
13. Chou, M. M., Hou, W., Johnson, J., Graham, L. K., Lee, M. H., Chen, C. S., Newton, A. C., Schaffhausen, B. S., and Toker, A. (1998) *Curr. Biol.* **8,** 1069–1077
14. Ikenoue, T., Inoki, K., Yang, Q., Zhou, X., and Guan, K. L. (2008) *EMBO J.* **27,** 1919–1931
15. Facchinetti, V., Ouyang, W., Wei, H., Soto, N., Lazorchak, A., Gould, C., Lowry, C., Newton, A. C., Mao, Y., Miao, R. Q., Sessa, W. C., Qin, J., Zhang, P., Su, B., and Jacinto, E. (2008) *EMBO J.* **27,** 1932–1943
16. Guertin, D. A., Stevens, D. M., Thoreen, C. C., Burds, A. A., Kalaany, N. Y., Moffat, J., Brown, M., Fitzgerald, K. J., and Sabatini, D. M. (2006) *Dev. Cell* **11,** 859–871
17. Keranen, L. M., Dutil, E. M., and Newton, A. C. (1995) *Curr. Biol.* **5,** 1394–1403
18. Behn-Krappa, A., and Newton, A. C. (1999) *Curr. Biol.* **9,** 728–737
19. Sonnenburg, E. D., Gao, T., and Newton, A. C. (2001) *J. Biol. Chem.* **276,** 45289–45297
20. Lee, H. W., Smith, L., Pettit, G. R., Vinitsky, A., and Smith, J. B. (1996) *J. Biol. Chem.* **271,** 20973–20976
21. Lu, Z., Liu, D., Hornia, A., Devonish, W., Pagano, M., and Foster, D. A. (1998) *Mol. Cell. Biol.* **18,** 839–845
22. Leontieva, O. V., and Black, J. D. (2004) *J. Biol. Chem.* **279,** 5788–5801
23. Gao, T., Brognard, J., and Newton, A. C. (2008) *J. Biol. Chem.* **283,** 6300–6311
24. Hansra, G., Bornancin, F., Whelan, R., Hemmings, B. A., and Parker, P. J. (1996) *J. Biol. Chem.* **271,** 32785–32788
25. Okuzumi, T., Fiedler, D., Zhang, C., Gray, D. C., Aizenstein, B., Hoffman, R., and Shokat, K. M. (2009) *Nat. Chem. Biol.* **5,** 484–493
26. Cameron, A. J., Escribano, C., Saurin, A. T., Kostelecky, B., and Parker, P. J. (2009) *Nat. Struct. Mol. Biol.* **16,** 624–630
27. Dutil, E. M., and Newton, A. C. (2000) *J. Biol. Chem.* **275,** 10697–10701
28. Srivastava, J., Goris, J., Dilworth, S. M., and Parker, P. J. (2002) *FEBS Lett.* **516,** 265–269
29. Sweatt, J. D., Atkins, C. M., Johnson, J., English, J. D., Roberson, E. D., Chen, S. J., Newton, A., and Klann, E. (1998) *J. Neurochem.* **71,** 1075–1085
30. Gallegos, L. L., Kunkel, M. T., and Newton, A. C. (2006) *J. Biol. Chem.* **281,** 30947–30956
31. Bishop, A. C., Buzko, O., and Shokat, K. M. (2001) *Trends Cell Biol.* **11,** 167–172
32. Hoshi, N., Langeberg, L. K., Gould, C. M., Newton, A. C., and Scott, J. D. (2010) *Mol. Cell* **37,** 541–550
33. Grodsky, N., Li, Y., Bouzida, D., Love, R., Jensen, J., Nodes, B., Nonomiya, J., and Grant, S. (2006) *Biochemistry* **45,** 13970–13981
34. Takimura, T., Kamata, K., Fukasawa, K., Ohsawa, H., Komatani, H., Yoshizumi, T., Takahashi, I., Kotani, H., and Iwasawa, Y. (2010) *Acta Crystallogr. D Biol. Crystallogr.* **66,** 577–583
35. Leonard, T. A., Różycki, B., Saidi, L. F., Hummer, G., and Hurley, J. H.

(2011) *Cell* **144,** 55–66

36. Davies, S. P., Reddy, H., Caivano, M., and Cohen, P. (2000) *Biochem. J.* **351,** 95–105
37. Gschwendt, M., Dieterich, S., Rennecke, J., Kittstein, W., Mueller, H. J., and Johannes, F. J. (1996) *FEBS Lett.* **392,** 77–80
38. Shi, F., Telesco, S. E., Liu, Y., Radhakrishnan, R., and Lemmon, M. A.

(2010) *Proc. Natl. Acad. Sci. U.S.A.* **107,** 7692–7697

39. Narayana, N., Diller, T. C., Koide, K., Bunnage, M. E., Nicolaou, K. C., Brunton, L. L., Xuong, N. H., Ten Eyck, L. F., and Taylor, S. S. (1999) *Biochemistry* **38,** 2367–2376
40. Akamine, P., Madhusudan, Wu, J., Xuong, N. H., Ten Eyck, L. F., and Taylor, S. S. (2003) *J. Mol. Biol.* **327,** 159–171